Supplement of Atmos. Chem. Phys., 18, 4069–4092, 2018
https://doi.org/10.5194/acp-18-4069-2018-supplement

Atmospheric Chemistry and Physics
Open Access
EGU

Supplement of

Abundance and sources of atmospheric halocarbons in the Eastern Mediterranean

Fabian Schoenenberger et al.

Correspondence to: Stephan Henne (stephan.henne@empa.ch)

Table S1: Basic statistics for the 3-hourly aggregates of the observations taken at all sites during the campaign period (Dec. 2012 – Aug.2013). Observation sites are: Finokalia (FKL), Jungfraujoch (JFJ), Mace Head (MHD), Monte Cimone (CMN). Shown are the number of observations (N), the mean, minimum (Min), maximum (Max) and standard deviation (SD) for the observations and the baseline values, estimated with REBS. The mean measurement uncertainty (σ_O) was determined from the standard deviation of reference gas measurements and the baseline uncertainty (σ_b) was derived as one constant value by the REBS method.

			Observations					Background (REBS)			
	Site	N	Mean [ppt]	Min [ppt]	Max [ppt]	SD [ppt]	σ_o [ppt]	Mean [ppt]	Min [ppt]	Max [ppt]	σ_b [ppt]
HFC-134a	FKL	1467	80.8	72.8	94.2	3.4	0.8	79.7	77.2	83.0	1.9
	JFJ	1383	80.7	70.9	119.3	5.3	0.2	77.0	74.6	79.1	1.3
	MHD	1533	80.3	73.5	122.0	5.6	0.2	77.4	76.3	78.9	0.7
	CMN	1040	86.1	72.8	129.3	8.7	0.3	80.1	76.2	83.1	1.7
HFC-125	FKL	1193	15.9	12.8	22.3	1.3	0.4	15.3	14.1	16.1	0.6
	JFJ	1373	16.1	13.3	26.9	1.7	0.1	14.9	14.1	15.7	0.3
	MHD	1514	15.8	13.9	28.1	1.7	0.1	14.9	14.5	15.4	0.2
	CMN	1078	17.6	13.4	33.3	2.6	0.1	15.8	14.6	16.8	0.6
HFC-152a	FKL	1428	11.5	7.8	19.3	1.6	0.2	10.6	10.3	10.7	0.8
	JFJ	1395	10.8	6.9	25.0	1.7	0.1	10.0	9.4	10.5	0.8
	MHD	1527	10.9	8.4	15.0	0.9	0.1	10.6	9.7	10.8	0.4
	CMN	1096	11.7	7.3	21.6	1.9	0.1	10.3	9.7	10.7	0.7
HFC-143a	FKL	1252	17.4	13.2	29.6	2.2	1.2	16.3	15.8	16.7	0.9
	JFJ	1411	16.7	13.7	25.6	1.6	0.1	15.4	14.5	16.0	0.3
	MHD	1540	16.6	14.8	27.6	1.8	0.1	15.5	15.3	15.9	0.2
	CMN	1055	17.5	14.2	27.1	1.9	0.1	16.0	15.1	16.8	0.5
HCFC-22	FKL	1438	235.8	226.9	271.6	3.5	1.8	234.7	233.0	237.9	2.3
	JFJ	1389	234.9	224.9	252.4	2.9	0.6	234.2	233.0	236.3	2.2
	MHD	1523	235.8	230.3	259.8	1.8	0.6	235.2	235.0	236.0	1.1
	CMN	980	235.1	225.2	255.5	3.3	0.7	234.0	232.2	235.8	1.9
HCFC-142b	FKL	1075	23.9	21.3	27.2	0.9	0.6	23.7	22.6	24.5	0.5
	JFJ	1392	23.4	22.4	26.1	0.4	0.1	23.2	23.1	23.4	0.2
	MHD	1533	23.3	22.7	24.7	0.2	0.1	23.2	23.1	23.3	0.1
	CMN	1046	23.8	22.5	26.8	0.5	0.1	23.5	23.2	23.8	0.3

Table S2: Inversion performance of the base inversion and the sensitivity inversions S-ML and S-MS for HFC-134a at Finokalia (FKL), Jungfraujoch (JFJ), Mace Head (MHD) and Monte Cimone (CMN). N is the number of observations used for the inversion. RMSE is the root mean square error in ppt (parts per billion 10^{-12}). R^2 denotes the coefficient of determination of the complete signals and R^2_{abg} is the coefficient of determination of the signals above background. TSS shows the Taylor Skill Score of the entire signal.

	Site	N	RMSE		R^2		R^2_{abg}		TSS	
			apriori	apost	prior	post	prior	post	prior	post
BASE	FKL	1421	4.7	1.7	0.41	0.74	0.20	0.29	0.86	0.95
	JFJ	1946	4.5	3.6	0.33	0.50	0.25	0.34	0.82	0.71
	MHD	2005	3.3	2.9	0.61	0.74	0.61	0.73	0.93	0.75
	CMN	1801	5.8	5.1	0.39	0.54	0.25	0.28	0.62	0.74
S-ML	FKL	1421	4.7	1.7	0.41	0.75	0.20	0.28	0.86	0.95
	JFJ	1946	4.5	3.6	0.33	0.50	0.25	0.32	0.82	0.68
	MHD	2005	3.3	3.3	0.61	0.68	0.61	0.68	0.93	0.66
	CMN	1801	5.8	5.1	0.39	0.55	0.25	0.28	0.62	0.73
S-MS	FKL	1421	4.7	1.7	0.41	0.75	0.20	0.36	0.86	0.97
	JFJ	1946	4.5	3.4	0.33	0.53	0.25	0.4	0.82	0.80
	MHD	2005	3.3	2.5	0.61	0.76	0.61	0.75	0.93	0.90
	CMN	1801	5.8	5.0	0.39	0.55	0.25	0.31	0.62	0.78

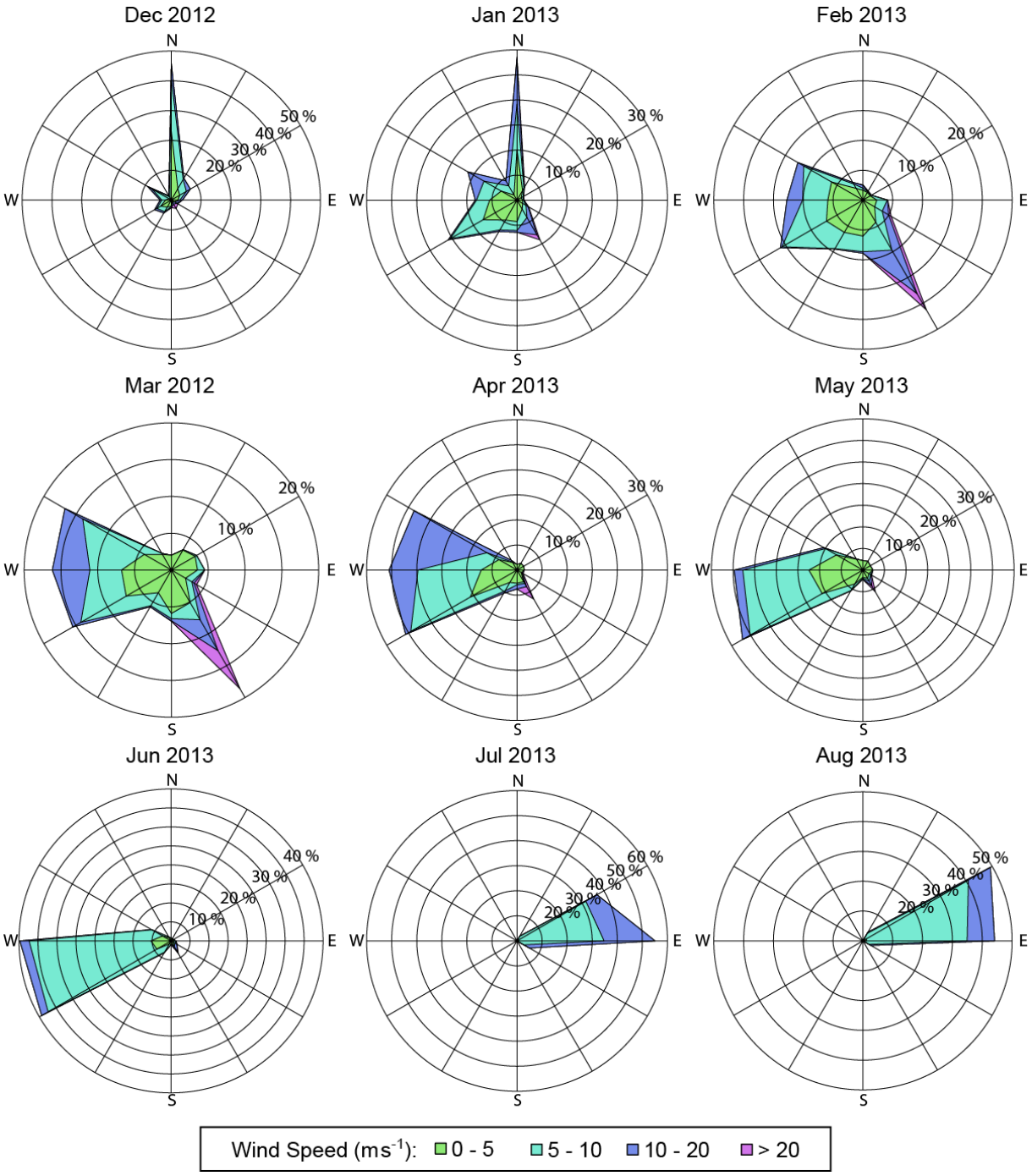

Figure S1: Observed monthly wind roses at Finokalia for the period January to August 2013 showing the directional frequencies colour-coded by wind speed based on 5 minute temporal resolution. Wind data were provided by the University of Crete.

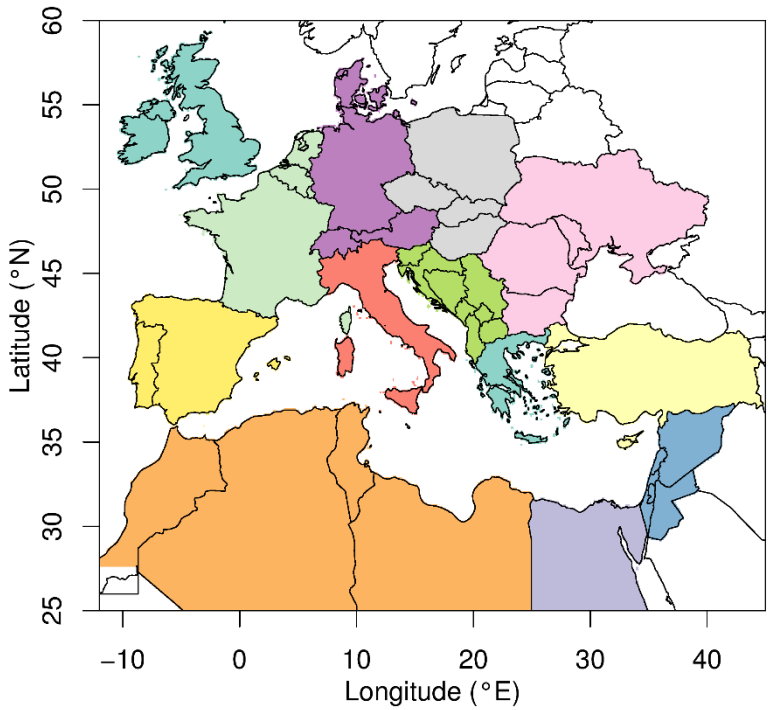

Figure S2: Illustration of region definition used in the discussion of emission estimates: Greece (light turquoise), Turkey (Turkey, Cyprus; pale yellow), Balkans (Serbia, Montenegro, Kosovo, Albania, Bosnia and Herzegovina, Croatia, Slovenia, Former Yugoslav Republic of Macedonia (FYROM); light green), Eastern (Ukraine, Romania, Moldova, Bulgaria; pale pink), Middle East (Jordan, Lebanon, Syria, Palestine, Israel; blue), Egypt (pale purple), Maghreb (Morocco, Algeria, Tunisia, Libya; orange), Central E (Poland, Slovakia, Czech-Republic, Hungary; grey), Central W (Switzerland, Liechtenstein, Germany, Austria, Denmark; purple), Western (France, Luxembourg, Netherlands, Belgium; pale green), Italy (red), Iberian Peninsula (Spain, Portugal; yellow), British Isles (Ireland, United Kingdom; light turquoise).

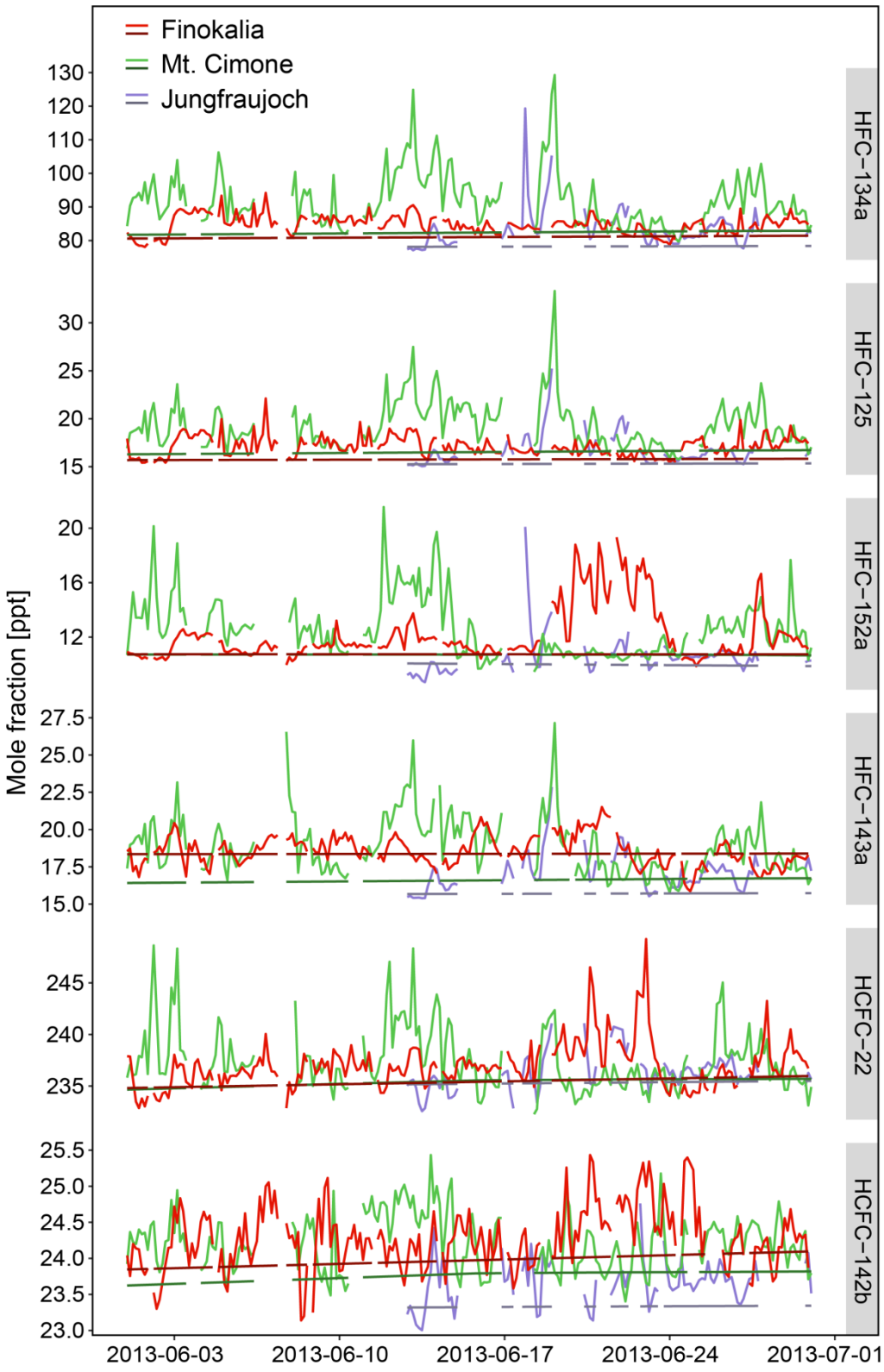

Figure S3: Halocarbon observations in June 2013 at Finokalia (red) and simultaneous measurements at Jungfraujoch (purple) and Monte Cimone (green). The corresponding background estimated with REBS is shown in the darker shade of the respective color.

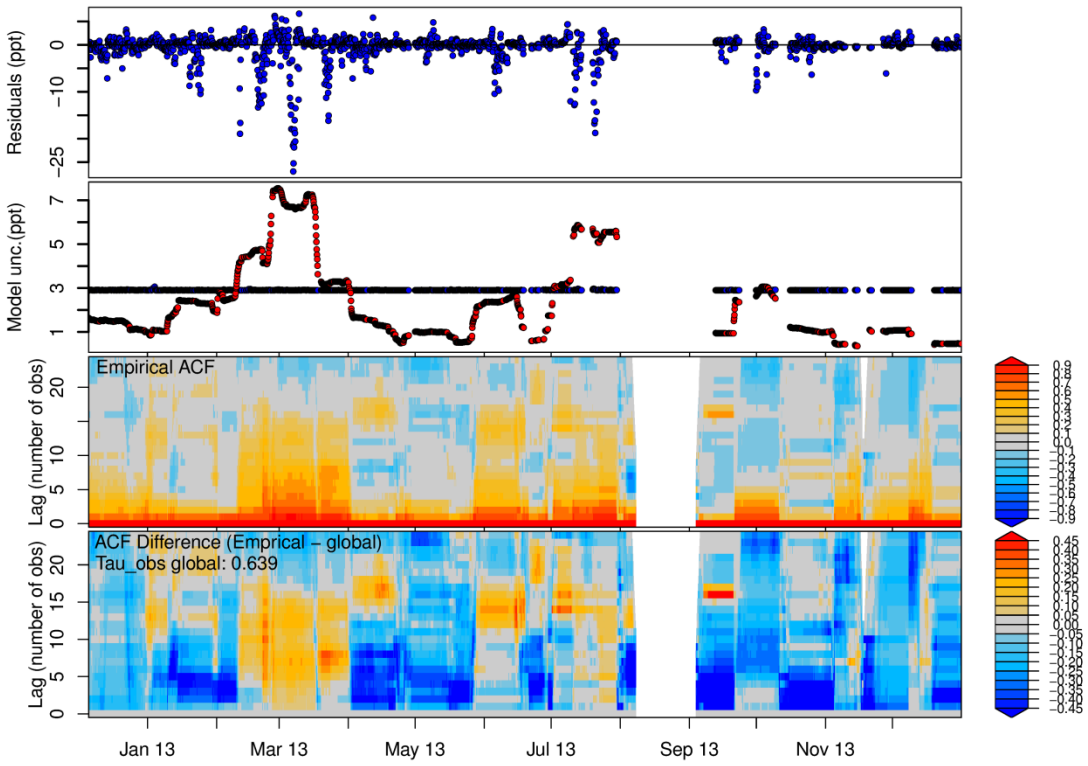

Figure S4: Time series of a) "prior" model residuals, b) data-mismatch uncertainty, blue symbols σ_c, and running RMS, red symbols, c) empirical auto correlation function based on 10 day moving window, d) difference between empirical ACF and fitted auto correlation function with constant (global) correlation length scale. All given for the site MHD and for HFC-134a.

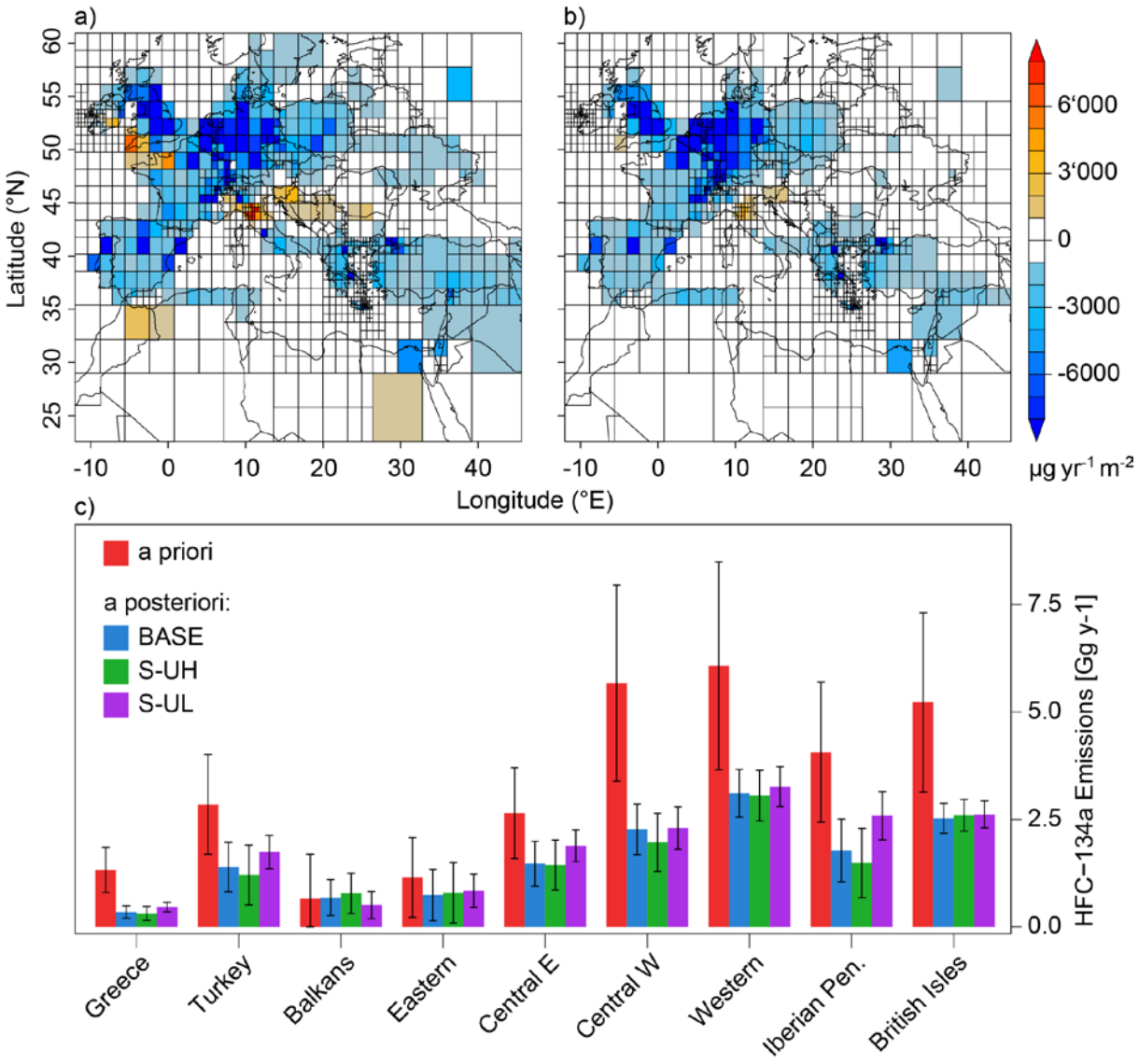

Figure S5: Difference of the a posteriori and a priori emissions for (a) the S-UH and (b) the S-UL inversions. (c) regional emission estimates: a priori emissions (red) and a posteriori emissions (BASE = blue, S-UH = green, S-UL = purple). The uncertainties given are two standard deviations of the analytic uncertainty assigned to the a priori emissions and derived by the inversion as a posteriori uncertainties.

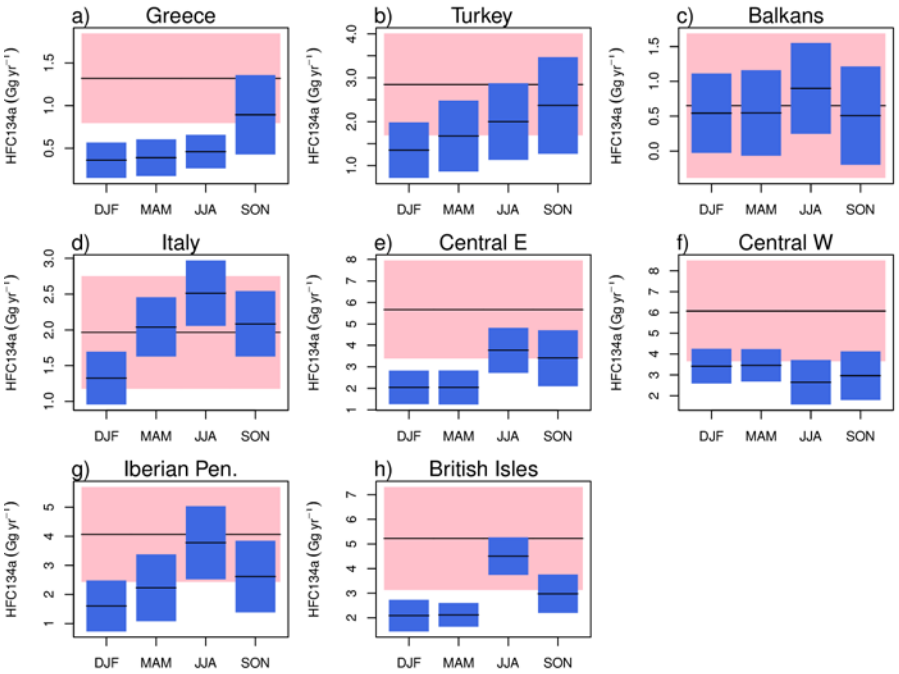

Figure S6: Seasonality of regional HFC-134a emission estimates: (red bars) a-priori and (blue bars) a posteriori emissions. The black lines give the mean estimates and the bars denote the uncertainty (1-σ level).